Int J Thermophys (2010) 31:199–207
DOI 10.1007/s10765-009-0696-x

Combined Photoacoustic–Acoustic Technique for Crack Imaging

J. Zakrzewski · N. Chigarev · V. Tournat · V. Gusev

Received: 31 March 2009 / Accepted: 15 December 2009 / Published online: 3 January 2010

Abstract Nonlinear imaging of a crack by combination of a common photoacoustic imaging technique with additional acoustic loading has been performed. Acoustic signals at two different fundamental frequencies were launched in the sample, one photoacoustically through heating of the sample surface by the intensity-modulated scanning laser beam and another by a piezoelectrical transducer. The acoustic signal at mixed frequencies, generated due to system nonlinearity, has been detected by an accelerometer. Different physical mechanisms of the nonlinearity contributing to the contrast in linear and nonlinear photoacoustic imaging of the crack are discussed.

Keywords Crack imaging · Nondestructive testing · Photoacoustics

1 Introduction

Localization of cracks on the initial stages of their creation and development is an important problem for nondestructive testing. Ultrasonic technique based on detection of scattering of sound waves by the crack is often not efficient for the detection of cracks. The reason is the presence of the acoustic background from the scattering of sound on the other inhomogeneities of the industrial samples, i.e., not on the cracks. The scattering from these irregularities usually covers the acoustic scattering from

J. Zakrzewski (✉) · N. Chigarev · V. Tournat
LAUM, CNRS, PRES UNAM, Université du Maine, Av. O. Messiaen, 72085 Le Mans, France
e-mail: jzakrzew@fizyka.umk.pl

J. Zakrzewski
Institute of Physics, Nicolaus Copernicus University, Grudziądzka 5/7, 87-100 Toruń, Poland

V. Gusev
LPEC, CNRS, PRES UNAM, Université du Maine, Av. O. Messiaen, 72085 Le Mans, France

the cracks. To avoid the problem of this background and improve the contrast of the defect localization, various nonlinear ultrasonic techniques have been proposed [1–3]. Acoustic nonlinearity can cause the appearance in the acoustic field spectrum of new frequency components, which are absent in the acoustic signal launched in the sample. These components are extremely sensitive indicators of the presence of the cracks and delaminations in the structure when the cracks and delaminations have much higher acoustic nonlinearity than an intact material, for example, in the cases where the acoustic field induces opening/closing of the contacts between the crack lips [3,4].

The photoacoustic imaging is based on the detection of the acoustic waves generated by a focused intensity-modulated laser beam scanning along the surface [5–7]. The amplitude of the acoustic signals generated by, for example, laser-induced thermoelastic expansion of a material depends on optical, thermal, and mechanical parameters of the material [7–9]. As a consequence of this, the photoacoustic images reflect the spatial inhomogeneity of one or of several of these parameters. Photoacoustic images reflecting the dependence of these parameters on laser intensity, temperature, or mechanical strain can be obtained by detecting the acoustic signals at such frequencies that are not launched in the system by laser-intensity modulation [10,11]. The contrast of these nonlinear photoacoustic images is expected to be higher than that of the linear images if the inhomogeneity of the nonlinear parameters of the material, based on the derivatives of the linear parameters, is higher than the inhomogeneity of the linear parameters.

Here, we report experimental results of photoacoustic imaging of a sample containing a surface breaking crack under the conditions of in-parallel additional loading of the sample by the acoustic field emitted by a piezoelectrical transducer. Our intention was to increase mechanical nonlinearity of the crack by inducing its motion in a highly nonlinear regime of opening/closing of the contacts between the lips of the crack and, thus, to increase the contrast of the nonlinear photoacoustic imaging of the crack. The existence of this regime is known from nonlinear acoustic experiments [4,12] and theory [13,14]. We were also interested to realize the imaging of the crack through the detection of acoustic waves at such mixed frequencies that are not launched in the system either by acoustical or photoacoustical excitation and are due to nonlinearity of the sample.

2 Experimental Setup

To observe the nonlinear frequency-mixing processes, the experimental setup shown in Fig. 1 has been prepared. The aluminum plate of $190 \times 20 \times 0.7\,\mathrm{mm}^3$ size was used as a sample. A crack in the plate was prepared by a fatigue machine with controllable stress. For imaging, this sample was deposited on a two-dimensional (2D) micro-translation stage controlled by a computer. To take advantage of the resonance acoustic properties of the sample, the metallic plate was acoustically isolated from the 2D stage by a porous material. The piezoelectric element of $\sim$100 kHz resonance frequency was glued on the surface of the sample. It was excited by a powerful generator with a voltage up to $\sim$100 V. To have a sufficiently large amplitude of the acoustic

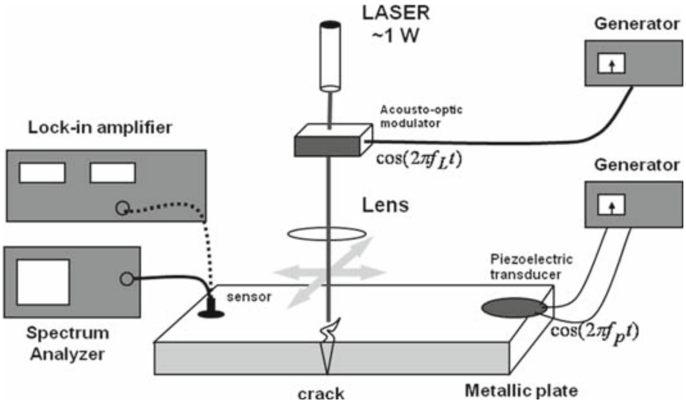

Fig. 1 Experimental photoacoustic-acoustic imaging setup. Metallic plate containing surface breaking crack is simultaneously excited by the piezoelectrical transducer at frequency f_P and through the absorption of cw laser radiation of intensity modulated at frequency f_L. Nonlinear photoacoustic images are obtained through the detection by the accelerometer or by the piezoelectric transducer of the acoustic waves at mixed frequency $f_L + f_P$ generated due to the nonlinearity of the crack

vibration, the resonance properties of the plates have been used. For this reason, the frequency of the piezoelectric excitation $f_P \sim 8.69$ kHz was chosen in the maximum of the highest amplitude resonance of the plate. For the photoacoustic excitation of the sample at frequency f_L, a continuous diode laser beam, intensity-modulated at frequency f_L by an acousto-optical modulator controlled by a radio-frequency generator, was used. It allowed obtaining a $P_L \sim 100$ mW power laser beam at ~800 nm wavelength with ~100 % modulation at f_L. The frequency of the modulation could be varied in the range from 10 Hz to 20 MHz. The modulated laser beam was focused on the surface of the sample by a lens with a focusing distance of ~5 cm into a spot ~200 μm in diameter. The absorption of the modulated laser radiation excites the acoustic waves in the plate as a result of the thermoelastic effect [8,9].

The acoustic vibrations of the plate were detected by means of an accelerometer (with up to ~100 kHz bandwidth) or a piezoelectric transducer (resonance frequency of 4 MHz). The sensors were glued on the surface of the plate under inspection at a distance of ~3 cm to 4 cm from the crack. The output of the sensors was amplified and connected to the input of a high-pass electronic filter. This filter was necessary to cut a strong electric signal at f_P and pass the components at f_L and at mixed frequencies. The output of the filter is connected to a spectrum analyzer of 10 MHz bandwidth or detected by a lock-in amplifier of 2 MHz maximum detection frequency.

3 Experimental Results

When the laser beam is focused in the vicinity of the crack, the experimental setup is used to measure accelerations of $10^3\ \mathrm{m \cdot s^{-2}}$ and $0.03\ \mathrm{m \cdot s^{-2}}$ in the acoustic waves excited by the piezoelectric transducer and by the modulated laser, respectively. The mechanical strains in the acoustic wave are estimated as 10^{-6} and 3×10^{-11},

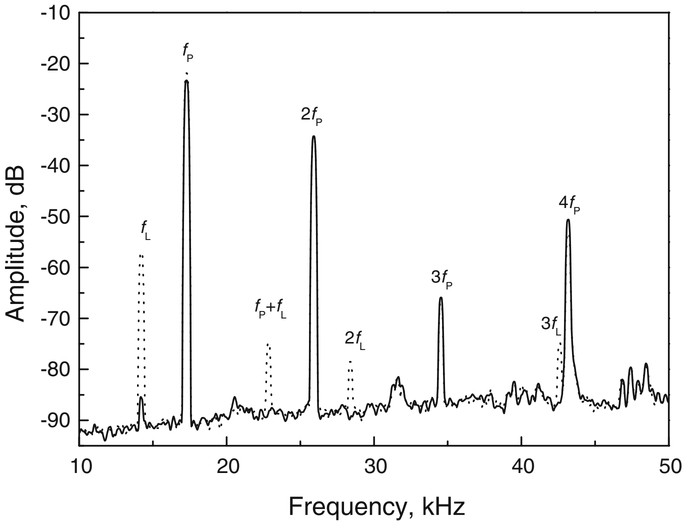

Fig. 2 Spectra of the plate vibrations. *Solid curve* is the spectrum of acoustic vibrations when the plate is excited at $f_P = 8.69$ kHz by piezo-transducer only. *Dashed curve* is the spectrum of acoustic vibrations when the plate is simultaneously excited by piezoelectrical transducer at $f_P = 8.69$ kHz and by cw laser with intensity modulated at $f_L = 14.28$ kHz

respectively. It is clear from these measurements conducted by an accelerometer at a distance ~4 cm from the crack that acoustic waves generated by the laser could participate in the nonlinear acoustic phenomena only if the laser is focused in the vicinity of the crack or, in other words, if the crack is located in the near field of the thermoelastic sound generator, where the amplitude of the acoustic waves at frequency f_L can be significantly higher. It is important to note that these measurements exclude the possibility of a contribution to nonlinear photoacoustic imaging of the mechanical nonlinearity of the contact between the powerful emitting piezoelectric transducer and the plate, because the amplitude of the photoacoustic signal at frequency f_L is too low in the vicinity of this contact.

The spectrum of the plate vibration obtained for the laser beam modulated at $f_L = 14.20$ kHz focused at the crack and the piezoelectric excitation at $f_P = 8.69$ kHz is shown in Fig. 2. The harmonics up to $4f_P$ for the piezoelectric transducer excited sound (solid curve) and up to $3f_L$ for the laser generated sound (dashed curve) are visible. It should be noted that a significant level of the harmonics in the spectrum of the photoacoustic signal is due mostly to the high level of their spurious presence in the spectrum of the laser-intensity envelope. As has been already mentioned, the frequency f_P of the piezoelectric excitation was chosen in the center of one of the resonances of the plate. In addition, the value of f_L was chosen through the maximization of the amplitude of the $f_P + f_L$ mixed frequency component in the spectrum in Fig. 2. The signal at $f_P + f_L$ is well seen in the spectrum (dashed curve). A priori, f_L was not chosen in the center of one of the plate resonances and was used as a tuning parameter for detection optimization.

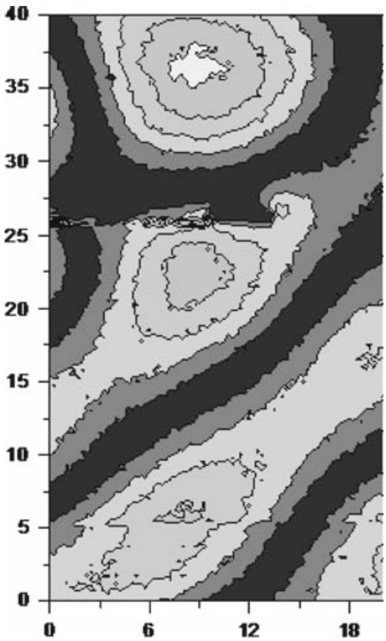

Fig. 3 2D photoacoustic image obtained by scanning of the laser foci on the surface of the plate with a size $20 \times 40\,\mathrm{mm}^2$. The signal was detected at the frequency of the laser intensity modulation ($f_\mathrm{L} = 72.68\,\mathrm{kHz}$). The change of color from *black* to *white* corresponds to the increase of the amplitude

2D distribution of the vibration amplitude at frequency f_L in the sample is shown in Fig. 3. It was obtained by scanning of the sample with the 2D stage, with the step of $\sim 0.1\,\mathrm{mm}$, to obtain the amplitude of the photoacoustic signal at the fundamental frequency. The periodical spatial structure of the acoustic standing mode is clearly seen. The distortions of the periodical picture could be related to the presence of the crack visible as a horizontal line near the coordinate $Y = 25$.

Figure 4 presents the dependence of the amplitude of the components of the photoacoustic signal spectrum at f_P, f_L, and $f_\mathrm{P} + f_\mathrm{L}$ on the voltage applied to the piezoelectric transducer. A characteristic diminishing of the amplitude of the acoustic signal at f_L, when the amplitude of the signal at f_P was increasing, has been observed. The diminishing of the signal at the frequency launched by the laser can be caused by the transmission of a part of the energy of this field to newly created frequencies. A similar effect was observed earlier in all-acoustical experiments on harmonics and subharmonics excitation [4].

Figure 5 shows the 2D images, obtained by 2D scanning by the laser foci in the vicinity of a crack, at the following frequencies: (a) and (d)—at fundamental frequency $f_\mathrm{L} = 20.12\,\mathrm{kHz}$ in the presence and in the absence of the piezoelectrical excitation, respectively; (b)—at mixed frequency $f_\mathrm{P} + f_\mathrm{L}$; and (c) and (e)—at second harmonic $2f_\mathrm{L}$ of the fundamental frequency f_L in the presence and in the absence of the piezoelectrical excitation, respectively.

The crack is visible in images (a) and (d) at the fundamental frequency f_L as a local increase of the optoacoustic signal in a spatial area with a size of $\sim 0.5\,\mathrm{mm}$ near the center of the images. The contrast of the images at the frequency f_L is related to inhomogeneity of linear parameters of the material controlling thermoelastic generation

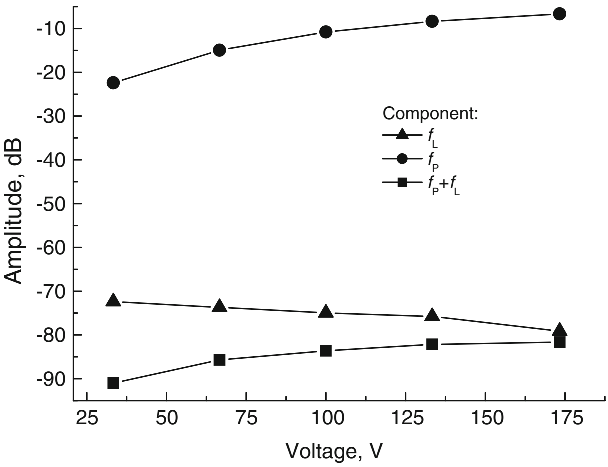

Fig. 4 Dependencies of the amplitude of the signals at the fundamental frequency of piezoelectrical excitation f_P, at the fundamental frequency of the laser-intensity modulation f_L, and at the mixed frequency $f_P + f_L$ on the amplitude of the voltage applied to the piezoelectrical element

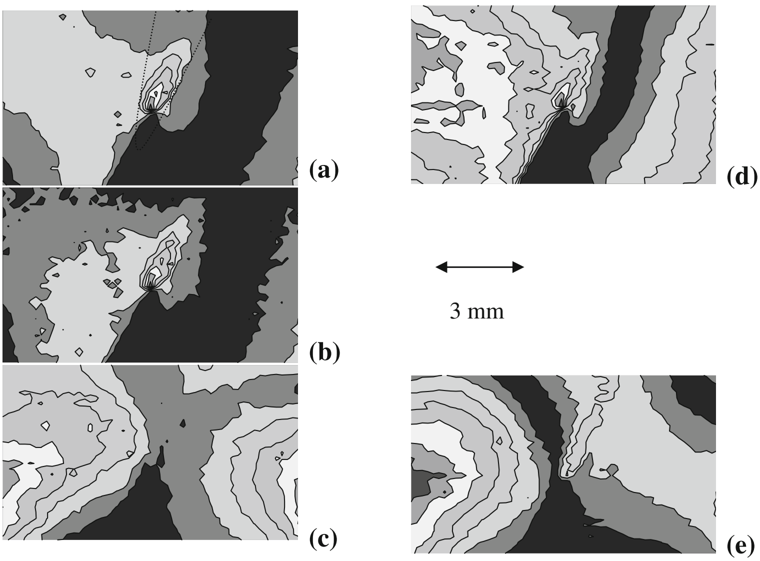

Fig. 5 2D images of the vicinity of the crack: (**a**) at the fundamental frequency f_L in the presence of the strong piezoelectrical excitation at frequency f_P, (**b**) at mixed frequency $f_L + f_P$, (**c**) at the second harmonic $2f_L$ of the laser-intensity modulation frequency in the presence of the strong piezoelectrical excitation at f_P, (**d**) at the fundamental frequency f_L without piezoelectrical excitation at frequency f_P, and (**e**) at the second harmonic $2f_L$ without strong piezo-excitation at the frequency f_P. The change of color from black to white corresponds to the increase of the amplitude. The crack is located within the region marked by the dotted line (**a**)

of sound. It is important to note here that the crack prepared in the aluminum plate was visible by eye. It means that this crack changes locally the optical properties of the plate and modifies the light absorption. Thus, in the considered case, the optical inhomogeneity introduced by the crack leads, together with the inhomogeneities of thermal and mechanical properties, to a corresponding variation of the linear photoacoustic signal in the vicinity of the crack. In Fig. 5a and d, a slow spatial variation of the signal with an amplitude comparable to the local increase of the signal amplitude near the crack can be associated with the spatial distribution of the amplitude in this vibrational mode of the plate. It is similar to one obtained previously for a larger area in another plate (Fig. 3). The difference between the images obtained at f_L in the presence (Fig. 5a) and in the absence (Fig. 5d) of the in-parallel piezoelectrical excitation can be attributed to modification of the average parameters of the material in the presence of intense acoustical loading due to the nonlinearity of the material (rectification or demodulation process [15,16]). In particular, the opening of the crack, i.e., its width, changes under intense acoustic loading [4,13,14].

A poor contrast of the images obtained at the second harmonic frequency $2f_L$ (Fig. 5c, e) can be caused by the presence of a significant level of the second harmonic in the spectrum of the intensity modulation of the incident laser beam. It is clear from Fig. 5b that the crack was visible at the mixed frequency $f_P + f_L$ with approximately the same spatial resolution as at the fundamental frequency f_L.

4 Physical Mechanisms of Nonlinear Frequency Mixing Processes

Several physical mechanisms already discussed in the literature can be responsible for the frequency-mixing processes in the vicinity of the crack. For the case of a high-amplitude piezoelectrically launched acoustic wave at f_P (pump wave) and a low-amplitude optically launched acoustic wave at f_L (probe wave) under the conditions of our experiments, the processes of frequency mixing can be conveniently viewed as the processes of parametric modulation of a weak probe wave by a strong pump wave.

The first physical mechanism is due to acoustic nonlinearity of the crack. Modulation of the crack opening (width) at frequency f_P by the strain of the pump acoustic wave will modulate at this frequency the reflection/transmission of the acoustic waves incident on the crack [2]. Consequently, the acoustic waves of frequency f_L incident on the crack will be additionally modulated in intensity at frequency f_P when being reflected by or transmitted through the gas-filled crack. This results in the appearance of the components $f_L + f_P$ and $f_L - f_P$ in the spectrum of the acoustic field.

The second mechanism is due to thermal nonlinearity of the crack [17–20]. Modulation of the crack opening at frequency f_P by the strain of the pump acoustic wave will modulate at this frequency the thermal resistance of the crack. For example, the thermal resistance of the thermally thin cracks is directly proportional to the crack width [18–20]. Consequently, the thermal waves of frequency f_L incident on the crack will be additionally modulated in intensity at frequency f_P when being reflected by or transmitted through the gas-filled crack. This results in the appearance of the components $f_L + f_P$ and $f_L - f_P$ in the spectrum of the temperature field. These mixed-frequency components of the temperature will generate the components $f_L + f_P$ and $f_L - f_P$ in the spectrum of the acoustic field through the thermoelastic effect.

The third mechanism worth mentioning here is due to optical nonlinearity of the crack [20]. Modulation of the crack opening at frequency f_P by the strain of the pump acoustic wave will modulate at this frequency a part of the laser field that penetrates through this opening inside the crack and, due to possible multiple scattering leading to partial capturing of this radiation inside the crack, is absorbed more efficiently than the laser radiation exhibiting just a single reflection at the intact surface of the sample. This results in modulation of the optical absorption in the vicinity of the crack at frequency f_P. Consequently, the absorbed laser radiation will exhibit additional modulation at this frequency in comparison with the incident laser radiation modulated at f_L only. The frequency components at $f_L + f_P$ and $f_L - f_P$ in the spectrum of the absorbed laser intensity envelope will induce the same spectral components in the temperature field through the heating effect, and the latter will generate the same spectral components of the acoustic field through the thermoelastic effect.

5 Discussion

The experimental observation that the contrast of the images at mixed frequency $f_L + f_P$ is similar to the contrast of linear images at frequency f_L, i.e., nonlinear imaging does not give important advantages in comparison with linear photoacoustic imaging indicates that the acoustic loading in our experiment was insufficiently high in amplitude to initiate strong nonlinearities of the crack expected when the contacts between the crack lips are opening/closing. In our experiments, a piezoelectrically launched acoustic wave caused only weak modulation of the crack opening leading to weak modulation of, for example, acoustical reflectivity of the crack, while in the case of opening/closing of the contacts between the crack lips the acoustic reflectivity can vary significantly (up to 100 % in the hypothetical limit of complete closing of the crack). The fact that nonlinear images of the crack do not have a high contrast indicate that in the experimentally realized regime the nonlinearities of the crack are not much higher than the nonlinearities of the intact material.

The nonlinear photoacoustic/acoustic imaging technique proposed here combines optical and acoustical methods of crack imaging. It should be noted that other nonlinear methods of nondestructive testing (detection) of the cracks also through the combination of optical and acoustical transducers have been reported earlier [21–24]. In [21,22], an optical interferometer was used for imaging of the nonlinear acoustic field created in the vicinity of the crack due to excitation of the sample by a very powerful transducer. In [23,24], the thermoelastic stresses produced by pulsed laser heating were used to induce opening/closing of the crack and to modulate the reflection of the surface acoustic waves monitored by an inter-digital transducer. In comparison with the method described here, the above-cited methods have both some advantages and some disadvantages. For example, in comparison with the first of them, the method proposed here does not require sufficiently high optical quality of the sample surface. In comparison with the second of them, the spatial resolution of the method proposed here is ultimately limited by the dimensions of the light absorption region and not by the acoustic wavelength.

6 Conclusions

Nonlinear imaging of a crack by a combination of a common photoacoustic imaging technique with additional acoustic loading has been performed. Acoustic signals at two different fundamental frequencies were launched in the sample, one photoacoustically through heating by the intensity-modulated scanning laser and another by a piezoelectrical transducer. The acoustic signal at mixed frequencies generated due to system nonlinearity has been detected by an accelerometer. The contrast of the images obtained at a mixed frequency is comparable with the obtained linear photoacoustic images, indicating that under the conditions of these experiments, optical, thermal, and acoustical nonlinearities of the surface breaking crack are not much higher than the nonlinearities of the intact material.

Acknowledgment The fellowship from CNRS France for Dr. J. Zakrzewski is gratefully acknowledged.

References

1. O. Buck, W.L. Morris, J.M. Richardson, Appl. Phys. Lett. **33**, 371 (1978)
2. J.G. Sessler, V. Weiss, *Crack Detection Apparatus and Method*, Patent US3867836, 1975
3. V.Yu. Zaitsev, V. Gusev, B. Castagnede, Phys. Rev. Lett. **89**, 105502 (2002)
4. A. Moussatov, V. Gusev, B. Castagnède, Phys. Rev. Lett. **90**, 124301 (2003)
5. G. Busse, A. Rosencwaig, Appl. Phys. Lett. **36**, 815 (1980)
6. Y.H. Wong, R.L. Thomas, J.J. Pouch, Appl. Phys. Lett. **35**, 368 (1979)
7. A. Rosencwaig, J. Appl. Phys. **51**, 2210 (1980)
8. A. Rosencwaig, *Photoacoustics and Photoacoustic Spectroscopy* (Wiley, New York, 1980)
9. V. Gusev, A. Karabutov, *Laser Optoacoustics* (AIP, New York, 1993)
10. Y.N. Rajakarunanayake, H.K. Wickramasinghe, Appl. Phys. Lett. **48**, 218 (1986)
11. G. Grégoire, V. Tournat, D. Mounier, V. Gusev, Eur. Phys. J. Spec. Topics **153**, 313 (2008)
12. I. Solodov, B. Korshak, Phys. Rev. Lett. **88**, 014303 (2002)
13. V. Gusev, B. Castagnède, A. Moussatov, Ultrasonics **41**, 643 (2003)
14. V. Gusev, J. Acoust. Soc. Am. **115**, 1044 (2004)
15. B.K. Novikov, O.V. Rudenko, V.I. Timochenko, *Nonlinear Underwater Acoustics* (ASA, New York, 1987)
16. V. Tournat, B. Castagnede, V. Gusev, P. Bequin, C.R. Mécanique **331**, 119 (2003)
17. G.C. Wetzel Jr., J.B. Spicer, Can. J. Phys. **64**, 1269 (1986)
18. V. Gusev, A. Mandelis, R. Bleiss, Appl. Phys. A **57**, 229 (1993)
19. V. Gusev, A. Mandelis, R. Bleiss, Mater. Sci. Eng. B **26**, 121 (1994)
20. J. Guitonny, V. Gusev, A.C. Boccara, D. Fournier, Prog. Nat. Sci. **6**, S-158 (1996)
21. N. Krohn, R. Stoessel, G. Busse, Ultrasonics **40**, 633 (2002)
22. I. Solodov, J. Wackerl, K. Pfleiderer, G. Busse, Appl. Phys. Lett. **84**, 5386 (2004)
23. H. Xiao, P.B. Nagy, J. Appl. Phys. **83**, 7453 (1998)
24. Z. Yan, P.B. Nagy, NDT & E Int. **33**, 213 (2000)